Facultad de Ciencias MATEMÁTICAS

UNIVERSIDAD COMPLUTENSE MADRID

Structures Beyond the Kuiper Cliff

Carlos de la Fuente Marcos ≡ Raúl de la Fuente Marcos

New Horizons Science Team Meeting #56: Open Session, May 15, 2024

AEGORA COMPLUTENSE RESEARCH GROUP ON SPACE ASTRONOMY AND DATA MINING

JcUVa

This research is the result of a collaboration by a team that includes:

Julia de León Cruz
Javier Licandro Goldaracena
Miquel Serra Ricart
Antonio Luis Cabrera Lavers

Ovidiu Văduvescu
Malin Stănescu

Facultad de Ciencias MATEMÁTICAS

One Slide Summary

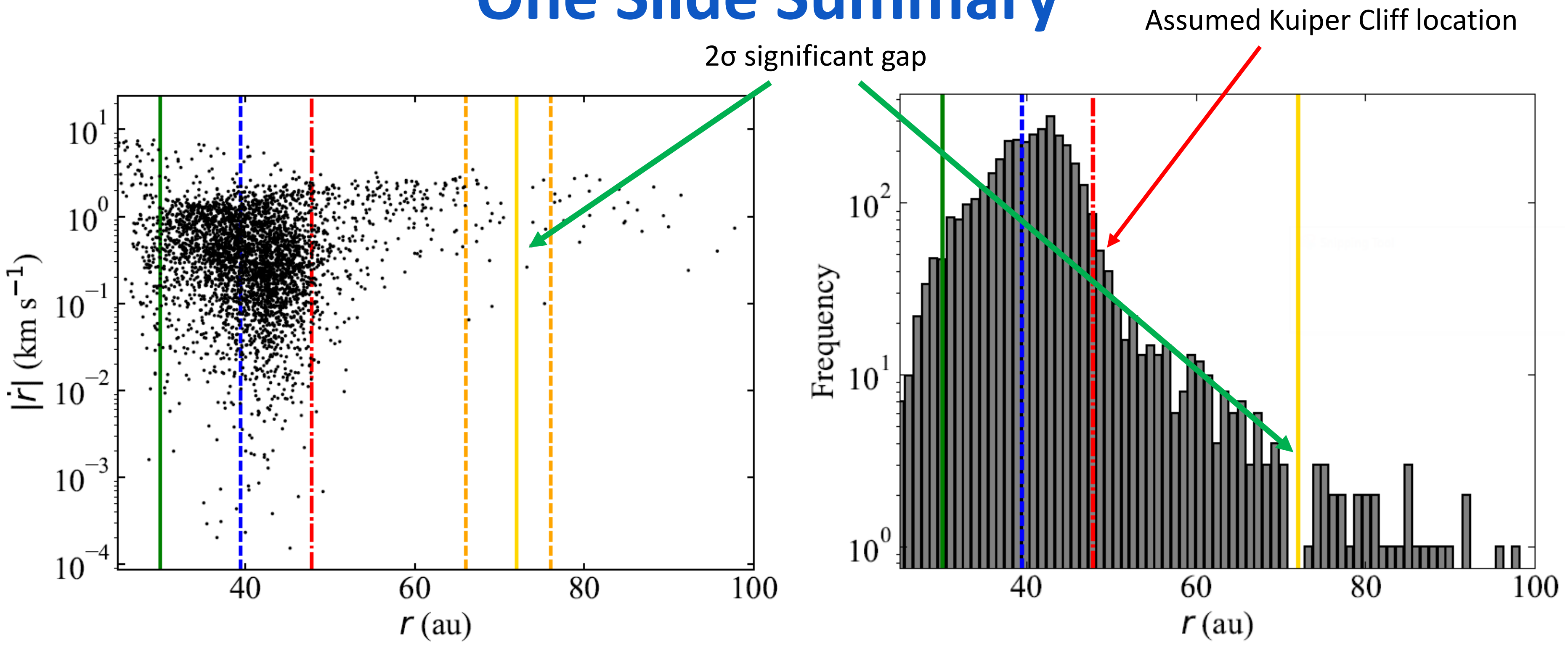

This research is an update of: MNRAS 527, L110–L114 (2024)

March 30, 1930: Pluto Is Discovered

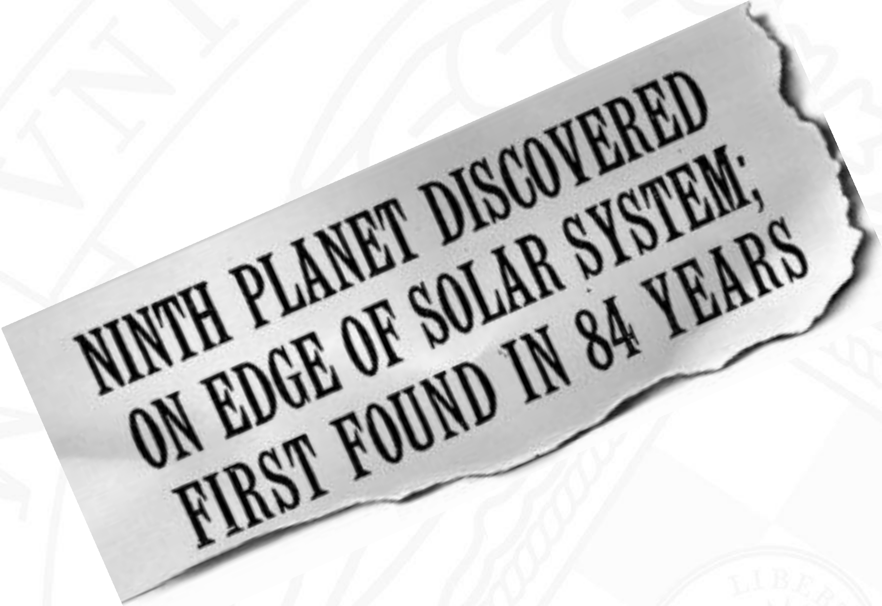

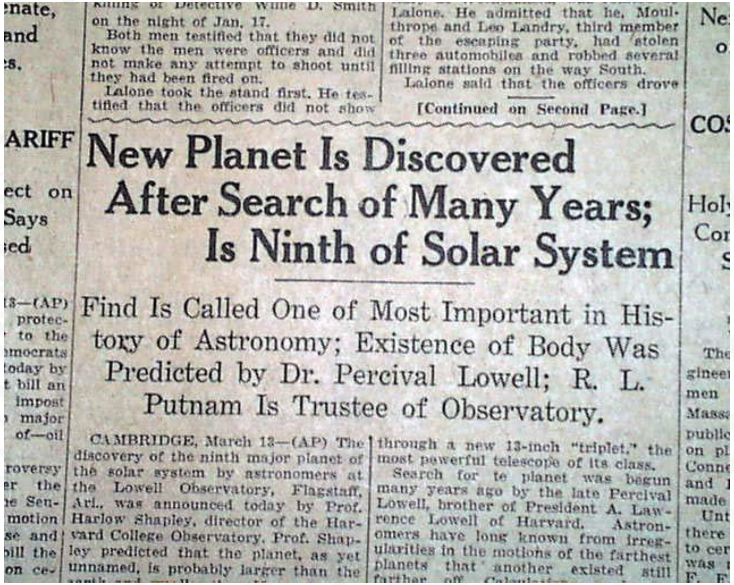

on the night of Jan. 17.
Both men testified that they did not know the men were officers and did not make any attempt to shoot until they had been fired on.
Lalone took the stand first. He testified that the officers did not show

Lalone. He admitted that he, Moulthrope and Leo Landry, third member of the escaping party, had stolen three automobiles and robbed several filling stations on the way South.
Lalone said that the officers drove

[Continued on Second Page.]

New Planet Is Discovered After Search of Many Years; Is Ninth of Solar System

Find Is Called One of Most Important in History of Astronomy; Existence of Body Was Predicted by Dr. Percival Lowell; R. L. Putnam Is Trustee of Observatory.

CAMBRIDGE, March 13—(AP) The discovery of the ninth major planet of the solar system by astronomers at the Lowell Observatory, Flagstaff, Ari., was announced today by Prof. Harlow Shapley, director of the Harvard College Observatory. Prof. Shapley predicted that the planet, as yet unnamed, is probably larger than the

through a new 13-inch "triplet," the most powerful telescope of its class.
Search for te planet was begun many years ago by the late Percival Lowell, brother of President A. Lawrence Lowell of Harvard. Astronomers have long known from irregularities in the motions of the farthest planets that another existed still

SIXTY-TWO YEARS LATER:

August 30, 1992: 15760 Albion (1992 QB_1) Is Discovered

Letter | Published: 22 April 1993

Discovery of the candidate Kuiper belt object 1992 QB_1

David Jewitt & Jane Luu

Nature 362, 730–732 (1993) | Cite this article

Abstract

THE apparent emptiness of the outer Solar System has been a long-standing puzzle for astronomers, as it contrasts markedly with the abundance of asteroids and short-period comets found closer to the Sun. One explanation for this might be that the orbits of distant objects are intrinsically short-lived, perhaps owing to the gravitational influence of the giant planets. Another possibility is that such objects are very faint, and thus they might easily go undetected. An early survey[1] designed to detect distant objects culminated with the discovery of Pluto. More recently, similar surveys yielded the comet-like objects 2060 Chiron[2] and 5145 Pholus[3] beyond the orbit of Saturn. Here we report the discovery of a new object, 1992 QB_1, moving beyond the orbit of Neptune. We suggest that this may represent the first detection of a member of the Kuiper belt[4,5], the hypothesized population of objects beyond Neptune and a possible source of the short-period comets[6–8].

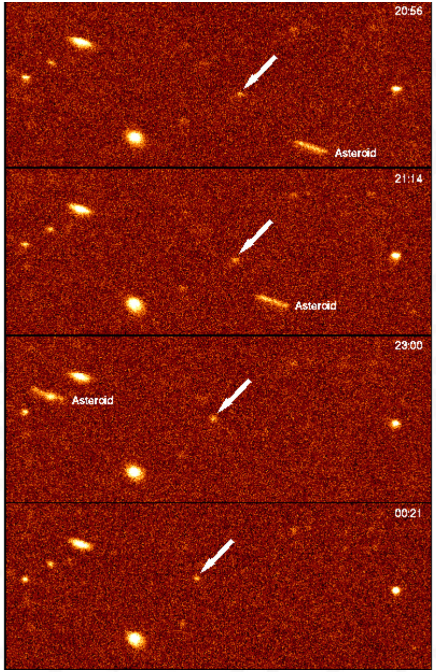

ELSEVIER

Icarus
Volume 157, Issue 2, June 2002, Pages 269-279

February 6, 2000: 148209 (2000 CR_{105}) Is Discovered

Regular Article

Evidence for an Extended Scattered Disk

B. Gladman [a], M. Holman [b], T. Grav [c], J. Kavelaars [d], P. Nicholson [e], K. Aksnes [c], J.-M. Petit [f]

Show more

+ Add to Mendeley   Share   Cite

https://doi.org/10.1006/icar.2002.6860

Get rights and content

Abstract

By telescopic tracking, we have established that the transneptunian object (TNO) 2000 CR_{105} has a semimajor axis of 220±1 AU and perihelion distance of 44.14±0.02 AU, beyond the domain which has heretofore been associated with the “scattered disk” of Kuiper Belt objects interacting via gravitational encounters with Neptune. We have also firmly established that the TNO 1995 TL_8 has a high perihelion (of 40.08±0.02 AU). These objects, and two other recent discoveries which appear to have perihelia outside 40 AU, have probably been placed on these orbits by a gravitational interaction which is *not* strong gravitational scattering off of any of the giant planets on their current orbits. Their existence may thus have profound cosmogonic implications for our understanding of the formation of the outer Solar System. We discuss some viable scenarios which could have produced these objects, including long-term diffusive chaos and scattering off of other massive bodies in the outer Solar System. This discovery implies that there must be a large population of TNOs in an “extended scattered disk” with perihelia above the previously suggested 38 AU boundary. The total population is difficult to estimate due to the ease with which such objects would have been lost. This illustrates the great value of frequent and well time-sampled recovery observations of trans-neptunian objects within their discovery opposition.

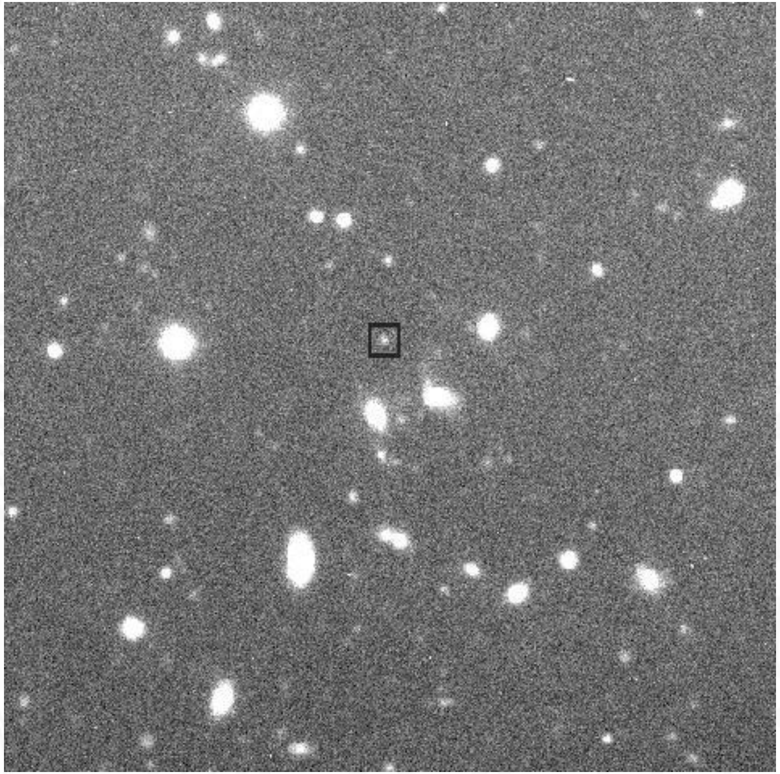

Facultad de Ciencias MATEMÁTICAS

The Astrophysical Journal, 617:645-649, 2004 December 10

Discovery of a Candidate Inner Oort Cloud Planetoid

Michael E. Brown
Division of Geological and Planetary Sciences, California Institute of Technology, Pasadena, CA 91125; mbrown@caltech.edu
Chadwick Trujillo
Gemini Observatory, 670 North A`ohoku Place, Hilo, HI 96720; trujillo@gemini.edu
and
David Rabinowitz
Department of Physics, Yale University, P.O. Box 208121, New Haven, CT 06520; david.rabinowitz@yale.edu

Received 2004 March 16; accepted 2004 April 21

ABSTRACT

We report the discovery of the minor planet (90377) Sedna, the most distant object ever seen in the solar system. Prediscovery images from 2001, 2002, and 2003 have allowed us to refine the orbit sufficiently to conclude that Sedna is on a highly eccentric orbit that permanently resides well beyond the Kuiper Belt with a semimajor axis of 480 ± 40 AU and a perihelion of 76 ± 4 AU. Such an orbit is unexpected in our current understanding of the solar system but could be the result of scattering by a yet-to-be-discovered planet, perturbation by an anomalously close stellar encounter, or formation of the solar system within a cluster of stars. In all of these cases a significant additional population is likely present, and in the two most likely cases Sedna is best considered a member of the inner Oort Cloud, which then extends to much smaller semimajor axes than previously expected. Continued discovery and orbital characterization of objects in this inner Oort Cloud will verify the genesis of this unexpected population.

November 14, 2003:
90377 Sedna (2003 VB_{12}) Is Discovered

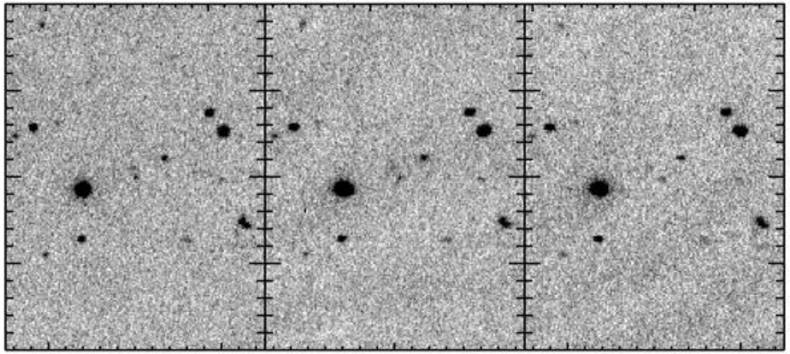

What is out there in the outskirts of known extrasolar planetary systems?

Extended Exo-Kuiper Belts

HD 104860
F8
100 au

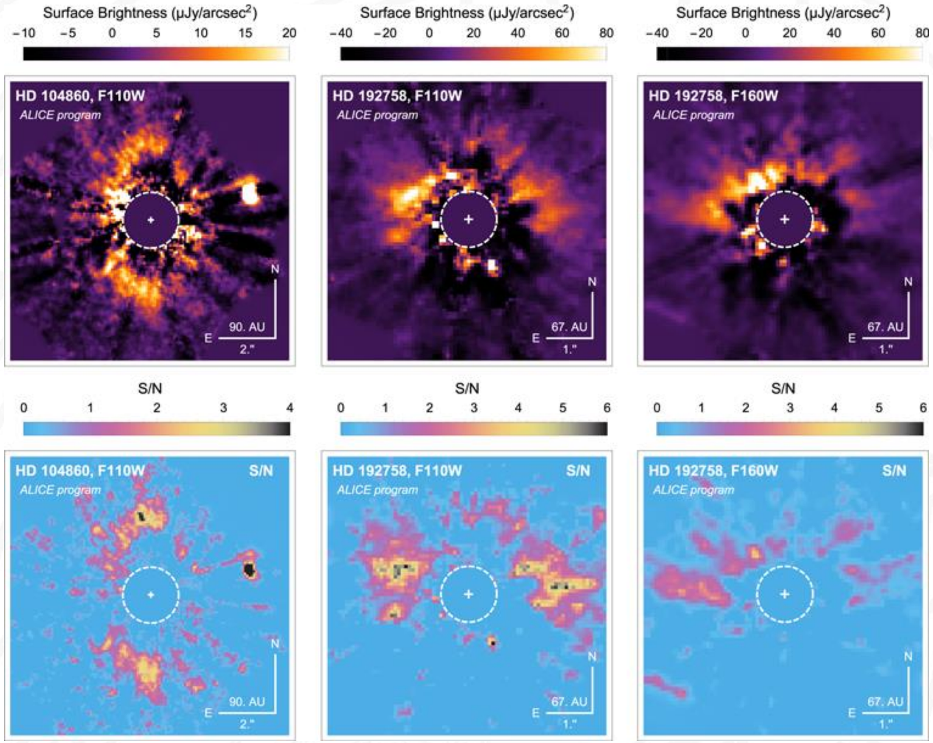

HD 192758
F0V
90 au

Extended Exo-Kuiper Belts

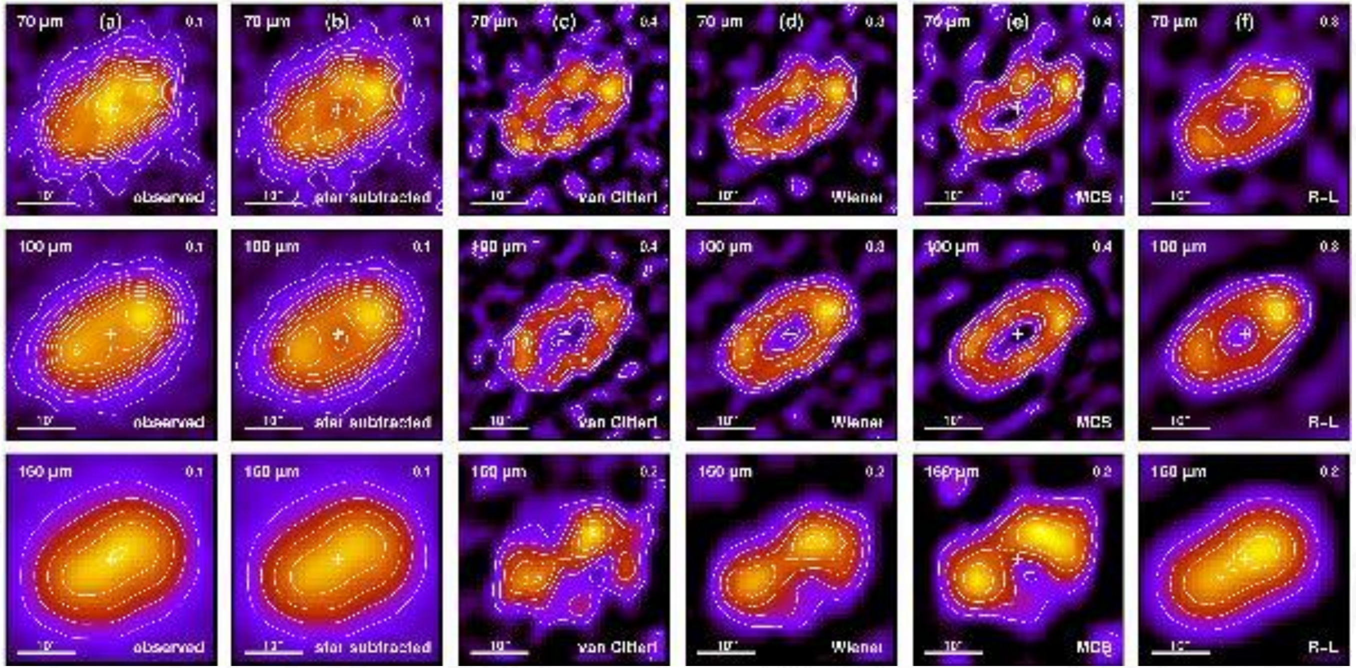

HD 207129

G0V

160 au

Distant worlds

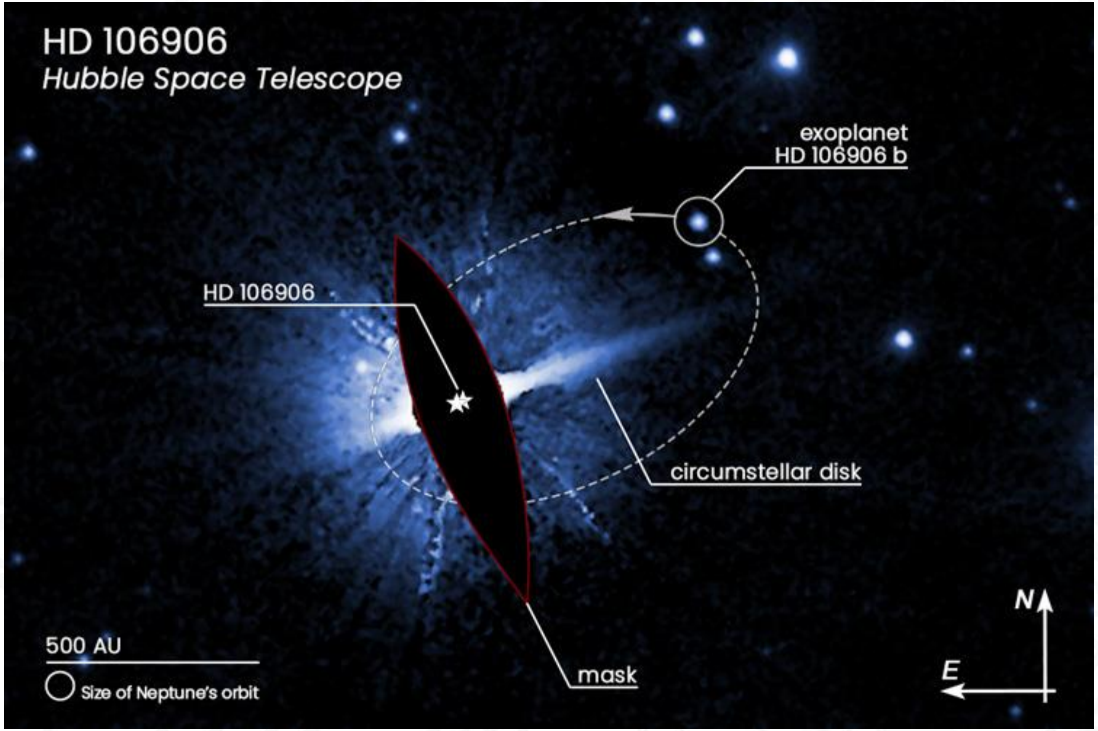

HD 106906
F5V
Exoplanet at 730 au
Belt out to 550 au

Candidates Here?

Exploring Trans-Neptunian Space with TESS: A Targeted Shift-stacking Search for Planet Nine and Distant TNOs in the Galactic Plane

Malena Rice[2,1] and Gregory Laughlin[1]

Published 2020 December 22 • © 2020. The Author(s). Published by the American Astronomical Society.
The Planetary Science Journal, Volume 1, Number 3
Citation Malena Rice and Gregory Laughlin 2020 *Planet. Sci. J.* **1** 81
DOI 10.3847/PSJ/abc42c

Article PDF | Article ePub

Figures ▾ Tables ▾ References ▾ Article data ▾

▾ Article and author information

Abstract

We present results from a new pipeline custom-designed to search for faint, undiscovered solar system bodies using full-frame image data from the NASA Transiting Exoplanet Survey Satellite (TESS) mission. This pipeline removes the baseline flux of each pixel before aligning and coadding frames along …sible orbital paths of interest. We first demonstrate the performance of the pipeline by recovering

Table 2
Candidates Recovered in Best-ever Frames Obtained with Both Baseline-subtraction Algorithms

N_{cand}	(S, Cam, CCD)	Cutout Origin	Type	R.A. (deg)	Decl. (deg)	$(\Delta x, \Delta y)$	V	d (au)	r (km)	N_{frames}	Epoch (JD)	Significance
1	(18, 2, 1)	(256, 384)	poly	43.9497	69.3189	(18, 1)	21.11	167.7	1517	573	2458810.25	9.29σ
			PCA	43.9497	69.3189	(18, 1)	21.15	167.7	1487	573	2458810.25	3.98σ
2	(18, 2, 3)	(0, 1664)	poly	16.6250	49.8912	(24, 4)	20.80	123.5	948	573	2458810.25	6.69σ
			PCA	16.6250	49.8912	(24, 4)	20.56	123.5	1060	573	2458810.25	4.31σ
3	(18, 3, 3)	(1280, 1664)	poly	344.4852	78.6428	(36, −3)	21.32	83.8	343	574	2458810.25	6.09σ
			PCA	344.5048	78.6538	(34, −3)	20.92	88.7	462	574	2458810.25	5.70σ
4	(18, 4, 2)	(1664, 1664)	poly	244.9781	73.4310	(32, 3)	22.05	95.6	320	574	2458810.25	6.96σ
			PCA	244.9781	73.4310	(32, 3)	21.70	95.6	375	574	2458810.25	5.24σ
		(1664, 1536)	poly	244.9781	73.4310	(32, 3)	22.04	95.5	321	574	2458810.25	7.20σ
			PCA	244.9781	73.4310	(32, 3)	21.69	95.5	376	574	2458810.25	5.21σ
5	(18, 4, 2)	(768, 1664)	poly	260.9884	70.8163	(32, 0)	22.16	96.3	309	574	2458810.25	5.21σ
			PCA	260.9884	70.8163	(32, 0)	21.43	96.3	375	574	2458810.25	3.91σ
		(768, 1792)	poly	260.9884	70.8163	(32, 0)	22.16	96.3	310	574	2458810.25	5.81σ
			PCA	260.9884	70.8163	(32, 0)	21.74	96.3	431	574	2458810.25	3.44σ
6	(18, 4, 3)	(1152, 1280)	poly	252.6156	65.2268	(38, 4)	22.06	80.7	227	574	2458810.25	6.03σ
			PCA	252.7973	65.2182	(37, 3)	21.4	83.1	319	574	2458810.25	3.91σ
7	(19, 2, 3)	(896, 1664)	poly	57.8788	61.6236	(36, 3)	20.74	106.7	727	539	2458838.92	5.73σ
			PCA	57.8788	61.6236	(36, 3)	20.20	106.7	933	539	2458838.92	3.95σ
8	(19, 3, 2)	(1664, 1024)	poly	122.2438	81.4212	(36, 0)	22.02	107.1	407	539	2458838.92	5.16σ
			PCA	122.2698	81.4253	(36, 3)	21.66	106.7	477	539	2458838.92	4.55σ
9	(19, 3, 2)	(896, 1536)	poly	105.0573	86.9216	(19, −2)	21.77	201.7	1616	539	2458838.92	7.07σ
			PCA	105.1514	86.9321	(19, 0)	21.62	202.8	1758	539	2458838.92	5.66σ
10	(19, 3, 2)	(1024, 1024)	poly	98.0576	83.7762	(42, 3)	21.89	91.5	316	539	2458838.92	5.74σ
			PCA	98.0063	83.7598	(42, 0)	21.48	91.8	384	539	2458838.92	5.02σ
11	(19, 3, 2)	(896, 1024)	poly	99.9219	83.7321	(23, 6)	21.92	162.1	976	539	2458838.92	5.76σ
			PCA	99.9219	83.7321	(23, 6)	21.59	162.1	1137	539	2458838.92	3.34σ
12	(19, 3, 2)	(1664, 1408)	poly	132.6612	82.2802	(30, 6)	21.85	126.0	608	539	2458838.92	6.06σ
			PCA	132.6612	82.2802	(30, 6)	21.65	126.0	667	539	2458838.92	4.53σ
13	(19, 3, 2)	(1408, 1664)	poly	140.7700	85.2651	(39, 5)	21.96	98.0	350	540	2458838.92	5.80σ
			PCA	140.7700	85.2651	(39, 5)	21.71	98.0	393	540	2458838.92	3.14σ
14	(19, 3, 3)	(640, 1280)	poly	206.4893	85.7287	(47, −3)	22.23	81.8	216	539	2458838.92	5.46σ
			PCA	206.3024	85.7390	(47, 0)	21.81	82.0	263	539	2458838.92	5.45σ
15	(19, 4, 1)	(1152, 1792)	poly	283.4931	66.3750	(32, 3)	21.91	119.9	538	540	2458838.92	5.19σ
			PCA	283.4931	66.3750	(32, 3)	21.40	119.9	679	540	2458838.92	3.33σ
16	(19, 4, 2)	(1408, 896)	poly	242,2779	73.2150	(42, 1)	22.04	91.7	295	539	2458838.92	6.17σ
			PCA	242,2779	73.2150	(42, 1)	21.62	91.7	359	539	2458838.92	5.22σ
17	(19, 4, 3)	(896, 1024)	poly	253.6466	60.7441	(45, −2)	22.20	85.6	240	539	2458838.92	5.33σ
			PCA	253.6466	60.7441	(45, −2)	21.85	85.6	282	539	2458838.92	3.04σ

Note. We report values recovered from both subtraction methods. Coordinates are reported at the last unmasked time in the sector, and the reported distances (d) refer to the predicted distance between the candidate object and the TESS spacecraft at the epoch of detection. For objects recovered in two separate stacks, four entries are included in the table, with results from the second stack provided as the third and fourth rows. Significances are reported as the deviation above zero flux recovered in our automated candidate extraction, where the standard deviation is calculated across the full best-ever frame.

Facultad de Ciencias MATEMÁTICAS

Candidates Here?

Monthly Notices of the ROYAL ASTRONOMICAL SOCIETY

MNRAS **513**, L78–L82 (2022) https://doi.org/10.1093/mnrasl/slac036
Advance Access publication 2022 April 8

Distant trans-Neptunian object candidates from NASA's TESS mission scrutinized: fainter than predicted or false positives?

C. de la Fuente Marcos [1]★ R. de la Fuente Marcos [2] O. Vaduvescu[3,4,5] and M. Stănescu[6]

[1]*Universidad Complutense de Madrid, Ciudad Universitaria, E-28040 Madrid, Spain*
[2]*AEGORA Research Group, Facultad de Ciencias Matemáticas, Universidad Complutense de Madrid, Ciudad Universitaria, E-28040 Madrid, Spain*
[3]*Isaac Newton Group (ING), Apt. de correos 321, E-38700 Santa Cruz de La Palma, Canary Islands, Spain*
[4]*Instituto de Astrofísica de Canarias (IAC), C/ Vía Láctea s/n, E-38205 La Laguna, Tenerife, Spain*
[5]*University of Craiova, Str. A. I. Cuza nr. 13, 200585 Craiova, Romania*
[6]*Bucharest Astroclub, Str. Cutitul de Argint 5, sector 4, Bucharest, 052034, Romania*

Accepted 2022 April 5. Received 2022 March 27; in original form 2022 March 6

ABSTRACT

NASA's *Transiting Exoplanet Survey Satellite* (*TESS*) is performing a homogeneous survey of the sky from space in search of transiting exoplanets. The collected data are also being used for detecting passing Solar system objects, including 17 new outer Solar system body candidates located at geocentric distances in the range 80–200 au, that need follow-up observations with ground-based telescope resources for confirmation. Here, we present results of a proof-of-concept mini-survey aimed at recovering two of these candidates that was carried out with the 4.2-m *William Herschel* Telescope and a QHY600L CMOS camera mounted at its prime focus. For each candidate attempted, we surveyed a square of over 1° × 1° around its expected coordinates in Sloan r'. The same patch of sky was revisited in five consecutive or nearly consecutive nights, reaching S/N > 4 at $r' < 23$ mag. We focused on the areas of sky around the circumpolar *TESS* candidates located at (07^h:00^m:15^s, +86°:55′:19″), 202.8 au from Earth, and (06^h:39^m:47^s, +83°:43′:54″) at 162.1 au, but we could not recover either of them at $r' \leq 23$ mag. Based on the detailed analysis of the acquired images, we confirm that either both candidates are much fainter than predicted or that they are false positives.

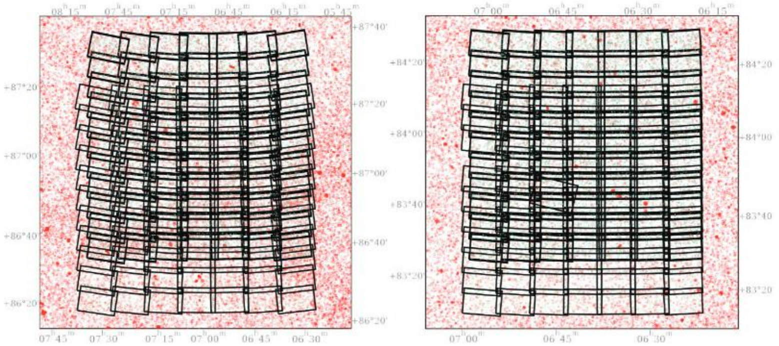

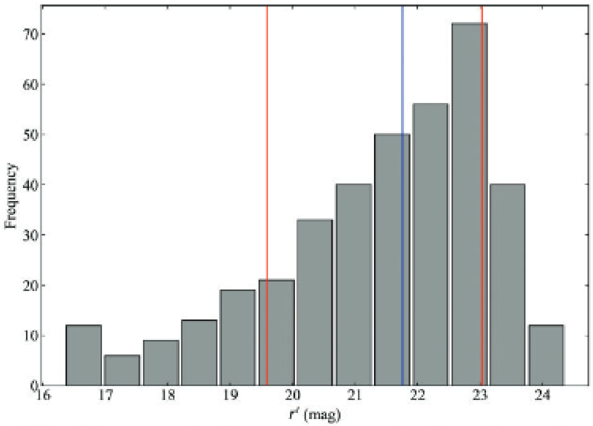

Candidates Here?

The Atacama Cosmology Telescope: A Search for Planet 9

Sigurd Naess[1], Simone Aiola[1], Nick Battaglia[2], Richard J. Bond[3], Erminia Calabrese[4], Steve K. Choi[2,5], Nicholas F. Cothard[5], Mark Halpern[6], J. Colin Hill[1,7], Brian J. Koopman[8]
Show full author list

Published 2021 December 23 •
The Astrophysical Journal, Volume 923, Number 2
Citation Sigurd Naess *et al* 2021 *ApJ* 923 224
DOI 10.3847/1538-4357/ac2307

Article PDF | Article ePub

Figures | Tables | References

Article and author information

Abstract

We use Atacama Cosmology Telescope (ACT) observations at 98 GHz (2015–2019), 150 GHz (2013–2019), and 229 GHz (2017–2019) to perform a blind shift-and-stack search for Planet 9. The search explores distances from 300 au to 2000 au and velocities up to 6$'$.3 per year, depending on the distance (r). For a 5 Earth-mass Planet 9 the detection limit varies from 325 au to 625 au, depending on the sky location. For a 10 Earth-mass planet the corresponding range is 425 au to 775 au. The predicted aphelion and most likely location of the planet corresponds to the shallower end of these ranges. The search covers the whole 18,000 square degrees of the ACT survey. No significant detections are found, which is used to place limits on the millimeter-wave flux density of Planet 9 over much of its orbit. Overall we eliminate roughly 17% and 9% of the parameter space for a 5 and 10 Earth-mass Planet 9, respectively. These bounds approach those of a recent INPOP19a ephemeris-based analysis, but do not exceed it. We also provide a list of the 10 strongest candidates from the search for possible follow-up. More generally, we exclude (at 95% confidence) the presence of an unknown solar system object within our survey area brighter than 4–12 mJy (depending on position) at 150 GHz with current distance 300 au < r < 600 au and heliocentric angular velocity $1'.5\,\mathrm{yr}^{-1} < v \cdot \frac{500\,\mathrm{au}}{r} < 2'.3\,\mathrm{yr}^{-1}$, corresponding to low-to-moderate eccentricities. These limits worsen gradually beyond 600 au, reaching 5–15 mJy by 1500 au.

Table 3
Top 10 Planet 9–Like Candidates, Sorted by the Detection Statistic z (see Section 4.7 or Appendix B for Definition)

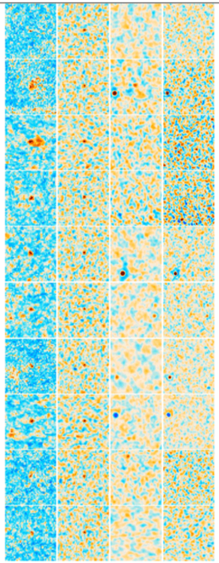

#	z map	Stack	f090	f150	R.A. (deg)	Decl. (deg)	z	F (mJy)	ΔF (mJy)	r (au)	v_x ($'$ yr^{-1})	v_y ($'$ yr^{-1})
1					−167.54	1.04	5.17	8.3	1.8	375	2.2	−2.9
2					−50.84	−9.16	5.05	11.5	2.4	375	0.2	3.0
3					−70.32	0.34	5.00	14.8	3.1	321	0.6	4.5
4					−150.37	−4.86	5.00	23.2	5.5	643	−0.1	−1.1
5					−179.17	−0.23	4.98	8.5	1.9	1125	0.0	0.4
6					179.01	4.34	4.92	6.3	1.4	500	1.3	−1.8
7					−173.55	15.20	4.92	4.1	0.9	346	−0.7	4.1
8					5.25	−0.70	4.87	5.6	1.3	643	−0.1	1.3
9					52.66	−2.60	4.87	10.1	2.3	563	−0.2	−1.7
10					−42.35	−45.80	4.87	8.4	1.7	500	0.3	1.8

Note. The columns are: #: the rank in terms of peak z value. **z map**: a thumbnail of the z map centered on the candidate. **Stack**: the shift-and-stack (i.e., motion-corrected) map for the best-fit parameters. **f090/f150**: filtered versions of the mean sky model in the f090/f150 band. Because these do not include any motion correction, no Planet 9 signal is expected here, but they are useful for seeing how "clean" each candidate's neighborhood is, e.g., if there are any bright point sources, dust clumps, or map edges at or near the candidate's location. All thumbnails are $45' \times 45'$ centered on the candidates. **R.A., decl.**: candidate's J2000 heliocentric equatorial coordinates on modified Julian day (MJD) 57688. **z**: the candidate's detection statistic z. F, ΔF: flux in the f150 band in mJy, assuming a 40 K blackbody, and its uncertainty. r: distance from the Sun, in au. v_x, v_y: intrinsic motion in arcminutes per year.

Table 4
Like Table 3, but for the General Candidates

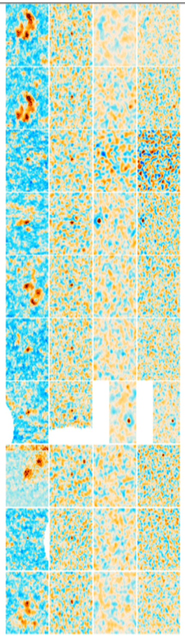

#	z map	Stack	f090	f150	R.A. (deg)	Decl. (deg)	z	F (mJy)	ΔF (mJy)	r (au)	v_x ($'$ yr^{-1})	v_y ($'$ yr^{-1})
1					−162.40	12.65	5.65	4.4	0.8	300	0.7	5.9
2					94.55	−29.48	5.64	9.7	1.8	500	1.6	1.5
3					116.58	−46.50	5.60	25.1	4.3	300	4.3	4.3
4					36.91	−12.81	5.51	13.7	3.4	1500	0.0	−0.1
5					59.20	1.52	5.48	11.3	2.4	643	0.6	0.6
6					69.03	−21.10	5.40	9.0	1.7	300	3.9	1.4
7					179.90	13.94	5.28	4.8	0.9	346	−3.7	−2.3
8					−8.19	−17.78	5.28	12.1	2.8	1125	−0.3	0.0
9					−69.90	−19.31	5.15	14.9	4.4	2000	0.0	0.1
10					−102.24	13.04	5.14	6.5	1.4	500	−1.4	−1.6

Candidates Here?

Unveiling the inert Oort cloud: Follow-up observations of ACT candidates with GTC/OSIRIS

Pencil-beam survey at various locations

Ongoing data analysis but so far null results

Breaking the 100 au Barrier

* The Solar System beyond 100 au from the Sun has only been studied using data provided by interplanetary probes like Voyager 1 and 2.

* The heliopause is located at about 120 au from the Sun and it is the region where the Solar wind meets the interstellar medium.

<u>* Distant trans-Neptunian objects (TNOs) are discovered by their *proper motion* that is mostly due to parallax.</u>

	r (au)	$\dot{r}$ (km/s)	
2018 AG_{37}:	132.5,	-0.11	(Subaru, Sheppard et al.)
2018 VG_{18}:	123.8,	0.27	(Subaru, Sheppard et al.)
2020 BE_{102}:	110.6,	-0.67	(Subaru, Sheppard et al.)
2020 MK_{53}:	159.8,	-0.04	(Subaru, Peltier et al. 2022; Fraser et al. 2023)

2018 VG18, Sheppard, S. S. et al., 2018, Minor Planet Electronic Circulars, 2018-Y14
2018 AG37, Sheppard, S. S. et al., 2021, Minor Planet Electronic Circulars, 2021-C187
2020 BE102, Sheppard, S. S. et al., 2022, Minor Planet Electronic Circulars, 2022-K172

Breaking the 100 au Barrier

Distances can be computed from the rate of motion that at opposition is:

$$\mu_{\text{opp}} = \frac{3547.2}{s + \sqrt{s}}$$

arcsec per day

Table 1. Apparent rate of motion at opposition and quadrature as a function of the heliocentric distance for objects moving in circular and coplanar (with Earth's) orbits.

s (au)	μ_{opp} (arcsec d^{-1})	μ_{qua} (arcsec d^{-1})
100	32.6	3.55
200	16.6	1.25
300	11.2	0.68
400	8.5	0.44
500	6.8	0.32
600	5.7	0.24
700	4.9	0.19
800	4.3	0.16
900	3.8	0.13
1000	3.4	0.11
1500	2.3	0.06
2000	1.7	0.04
3000	1.2	0.02
4000	0.9	0.01
5000	0.7	0.01

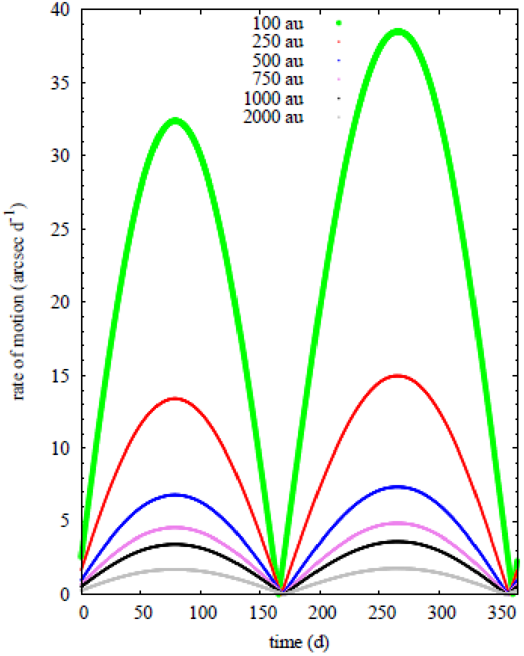

Breaking the 100 au Barrier

* The orbit determinations of distant objects based on data arcs shorter than about a year are very unreliable and their associated uncertainties could be very large.

* However, their geocentric, heliocentric or barycentric distances estimated for an epoch chosen between the dates of their first and last observation could be uncertain by a few percent.

When discovered, the only reliable parameters of the distant object candidates are their range (r) and range-rate ($\dot{r}$). Low values of the range-rate signal perihelion/aphelion.

$$\mu_{\mathrm{opp}} = \frac{3547.2}{s + \sqrt{s}}$$

arcsec per day

Informal Citizen Science

* The orbit determinations of distant objects can only be improved by increasing the data-arc span, but distant objects have orbital periods of thousands of years.

* Precoveries are observations of known objects that pre-date the discovery date. Finding precoveries helps improving orbit determinations without having to wait for decades to get more data.

Large numbers of public, undocumented archive images exist on-line. Most successful precoveries are carried out by amateur sleuths (in some cases pre-teens or teenagers).

Data Mining for TNOs

The values of the range and range-rate of newly discovered TNOs are reliable, but their orbits are not. These values of range and range-rate and their uncertainties can be obtained via the astroquery Python package from JPL's Horizons.

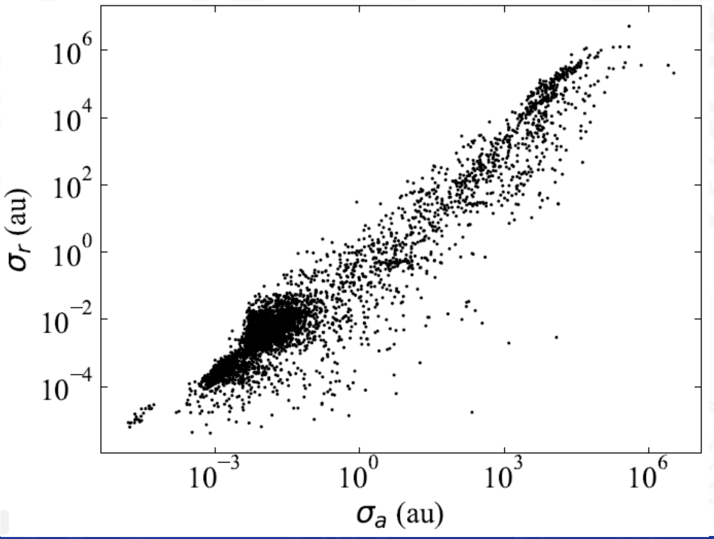

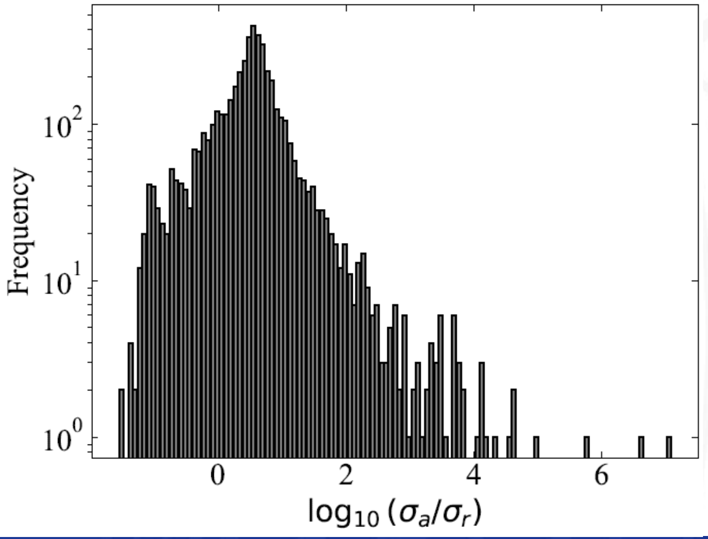

Facultad de Ciencias MATEMÁTICAS

The Kuiper Cliff is often placed at the 1:2 mean-motion resonance with Neptune at 47.8 au

Keck Pencil-Beam Survey for Faint Kuiper Belt Objects

E. I. Chiang[1] and M. E. Brown[1,2]

The Astronomical Journal, Volume 118, Number 3

Citation E. I. Chiang and M. E. Brown 1999 AJ 118 1411

DOI 10.1086/301005

Article PDF | View article

References

Article and author information

Abstract

We present the results of a pencil-beam survey of the Kuiper Belt using the Keck 10 m telescope. A single 0.01 deg^2 field is imaged 29 times for a total integration time of 4.8 hr. Combining exposures in software allows the detection of Kuiper Belt objects (KBOs) having visual magnitude $m_V \lesssim 27.9$. Two new KBOs are discovered. One object having $m_V = 25.5$ lies at a probable heliocentric distance $R \approx 33$ AU. The second object at $m_V = 27.2$ is located at $R \approx 44$ AU. Both KBOs have diameters of about 50 km, assuming comet-like albedos of 4%. Data from all surveys are pooled to construct the luminosity function from $m_R = 20$ to 27. The cumulative number of objects per square degree, $\Sigma(<m_R)$, is fitted to a power law of the form $\log_{10} \Sigma = \alpha(m_R - 23.5)$, where the slope $\alpha = 0.52 \pm 0.02$. Differences between slopes reported in the literature are due mainly to which survey data are incorporated in the fit and not to the method of analysis. The luminosity function is consistent with a power-law size distribution for objects having diameters $s = 50$–500 km within 50 AU; $dN \propto s^{-q}\, ds$, where the differential size index $q = 3.6 \pm 0.1$. We estimate to order of magnitude that $0.2\, M_\oplus$ and 1×10^{10} comet progenitors lie between 30 and 50 AU. Though our inferred size index nearly matches that derived by Dohnanyi, it is unknown whether catastrophic collisions are responsible for shaping the size distribution. Impact strengths may increase strongly with size from 50 to 500 km, whereas the derivation by Dohnanyi assumes impact strength to be independent of size. Collisional lifetimes of KBOs having diameters 50–500 km exceed the age of the solar system by at least 2 orders of magnitude in the present-day Belt, assuming bodies consist of solid, cohesive rock. Implications of the absence of detections of classical KBOs beyond 50 AU are discussed.

Using the values of the range of the TNOs instead of their orbits was first considered by Trujillo & Brown (2001)

The Radial Distribution of the Kuiper Belt

Chadwick A. Trujillo[1] and Michael E. Brown[1]

Published 2001 May 31 •

The Astrophysical Journal, Volume 554, Number 1

Citation Chadwick A. Trujillo and Michael E. Brown 2001 *ApJ* 554 L95

DOI 10.1086/320917

Article PDF   View article

References

Article and author information

Abstract

We examine the radial distribution of the Kuiper Belt objects (KBOs) using a method that is insensitive to observational bias effects. This technique allows the use of the discovery distances of all KBOs, independent of orbital classification or discovery circumstance. We verify the presence of an outer edge to the Kuiper Belt, as reported in other works, and we measure this edge to be at R = 47 ± 1 AU given any physically plausible model of the size distribution. We confirm that this outer edge is due to the classical KBOs, the most numerically dominant observationally. In addition, we find that current eys do not preclude the presence of a second, unobserved Kuiper Belt beyond R = 76 AU.

Facultad de Ciencias
MATEMÁTICAS

MNRAS 527, L110–L114 (2024)

Sample size: 4474

Monthly Notices of the ROYAL ASTRONOMICAL SOCIETY

MNRAS **527**, L110–L114 (2024) https://doi.org/10.1093/mnrasl/slad132
Advance Access publication 2023 September 20

Past the outer rim, into the unknown: structures beyond the Kuiper Cliff

C. de la Fuente Marcos[1★] and R. de la Fuente Marcos[2]
[1]*Universidad Complutense de Madrid, Ciudad Universitaria, E-28040 Madrid, Spain*
[2]*AEGORA Research Group, Facultad de Ciencias Matemáticas, Universidad Complutense de Madrid, Ciudad Universitaria, E-28040 Madrid, Spain*

Accepted 2023 September 15. Received 2023 September 14; in original form 2023 August 11

ABSTRACT

Although the present-day orbital distribution of minor bodies that go around the Sun between the orbit of Neptune and the Kuiper Cliff is well understood, past ∼50 au from the Sun, our vision gets blurred as objects become fainter and fainter and their orbital periods span several centuries. Deep imaging using the largest telescopes can overcome the first issue but the problems derived from the second one are better addressed using data analysis techniques. Here, we make use of the heliocentric range and range-rate of the known Kuiper belt objects and their uncertainties to identify structures in orbital parameter space beyond the Kuiper Cliff. The distribution in heliocentric range there closely resembles that of the outer main asteroid belt with a gap at ∼70 au that may signal the existence of a dynamical analogue of the Jupiter family comets. Outliers in the distribution of mutual nodal distances suggest that a massive perturber is present beyond the heliopause.

Key words: methods: data analysis – celestial mechanics – Kuiper belt: general – minor planets, asteroids: general.

1 INTRODUCTION

The Solar system beyond Neptune was a great unknown when (134340) Pluto 1930 BM was discovered by C. W. Tombaugh (Aitken 1930). It was soon suggested that a population of bodies in Pluto-like orbits existed beyond Neptune (Leonard 1930) and this hypothesis was independently explored by several authors (see e.g. Edgeworth 1943, 1949; Kuiper 1951; Cameron 1962, 1978; Whipple 1964, 1972; Fernandez 1980). The credibility of this conjecture was confirmed numerically by Duncan, Quinn & Tremaine (1988), but the observational proof had to wait until 1992 when the second member of this population, (15760) Albion 1992 QB_1 was found (Jewitt, Luu & Marsden 1992; Jewitt & Luu 1993).

from the best sample. Our results are discussed in Section 6 and our conclusions are summarized in Section 7.

2 DATA AND TOOLS

In this work, we use ephemerides computed by Jet Propulsion Laboratory's (JPL) Horizons online Solar system data and ephemeris computation service[1] (Giorgini 2015) that utilizes the new DE440/441 general-purpose planetary solution (Park et al. 2021). Data queries were made via the PYTHON package ASTROQUERY (Ginsburg et al. 2019). Our input data sample was retrieved from JPL's Small-Body Database (SBDB).[2] It includes all the 4474 objects (as of 2023 Aug 30) in the trans-Neptunian object orbit class (semimajor axis, *a*

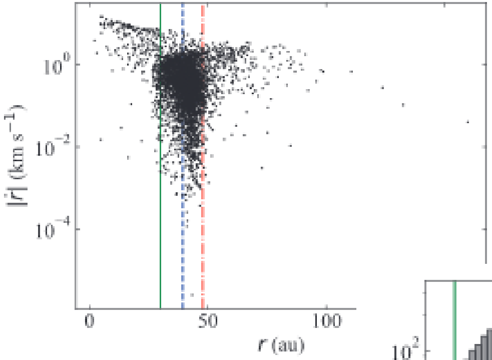

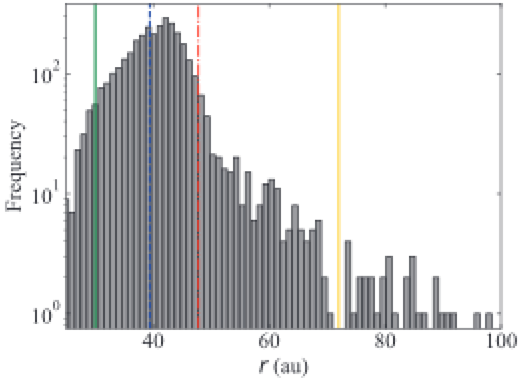

NEW ANALYSIS: DATA AS OF MAY 14, 2024, SAMPLE SIZE 4759

KUIPER BELT

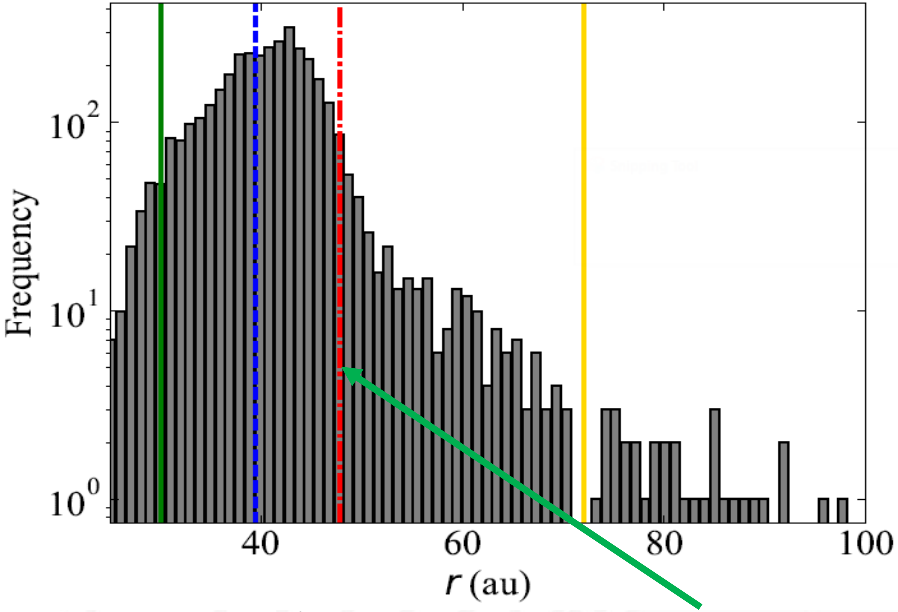

OUTER MAIN ASTEROID BELT

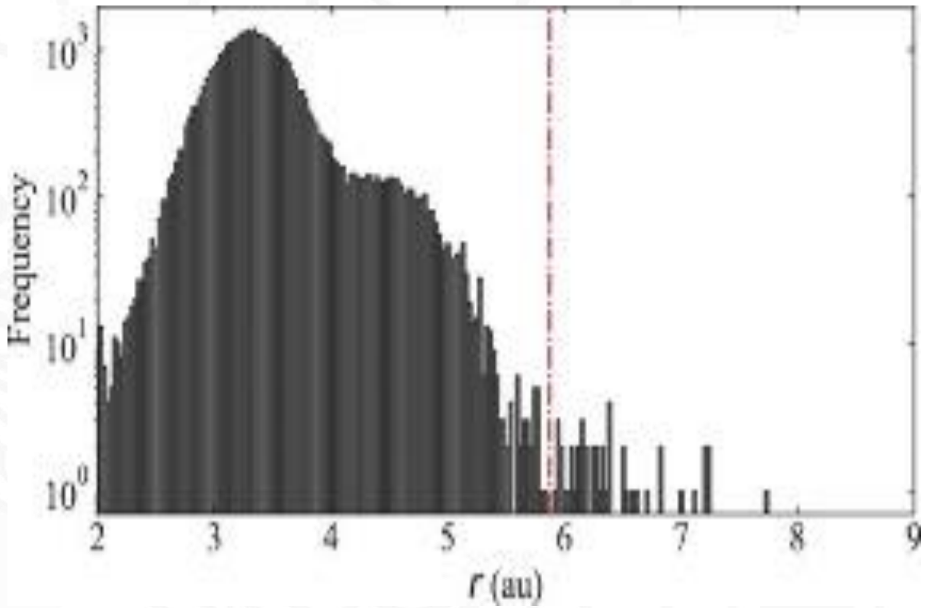

The location of the 1:1 mean-motion resonance with Neptune at 30.0 au is displayed as a green solid vertical line, the 2:3 resonance at 39.4 au as blue dashed, and the 1:2 resonance at 47.8 au as red dot–dashed.

Histograms use a bin width computed by applying the Freedman–Diaconis rule (Freedman & Diaconis 1981)

NEW ANALYSIS: DATA AS OF MAY 14, 2024, SAMPLE SIZE 4759

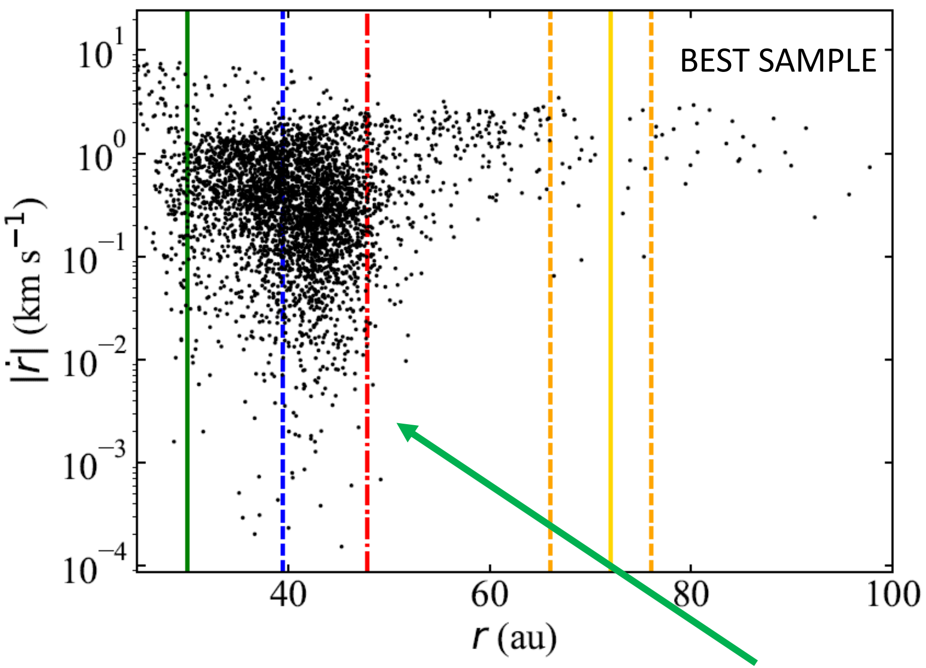

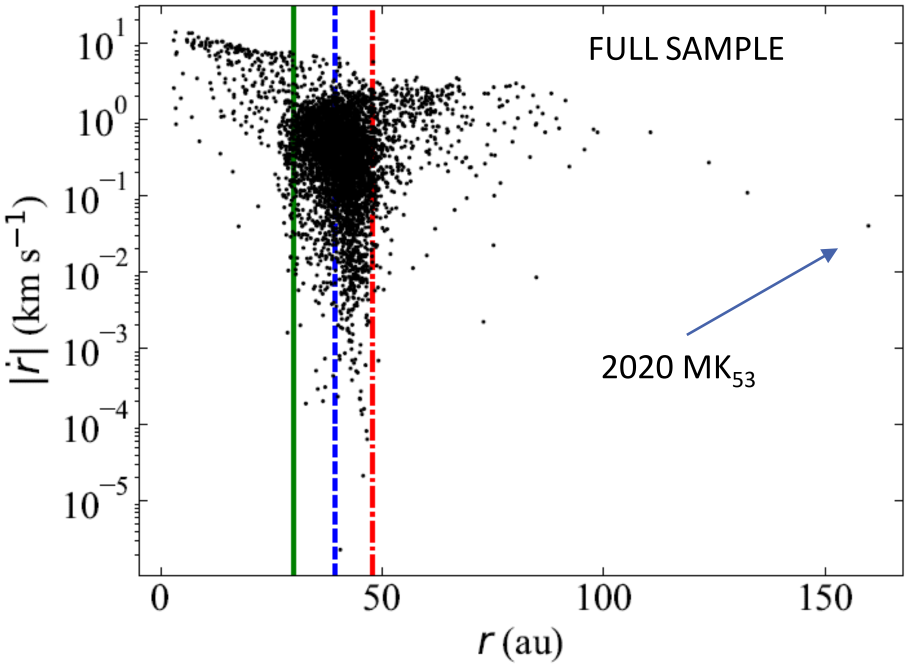

The location of the 1:1 mean-motion resonance with Neptune at 30.0 au is displayed as a green solid vertical line, the 2:3 resonance at 39.4 au as blue dashed, and the 1:2 resonance at 47.8 au as red dot–dashed.

Origin of the Observed Substructure

Distribution of mutual nodal distances

EXTREME TRANS-NEPTUNIAN OBJECTS

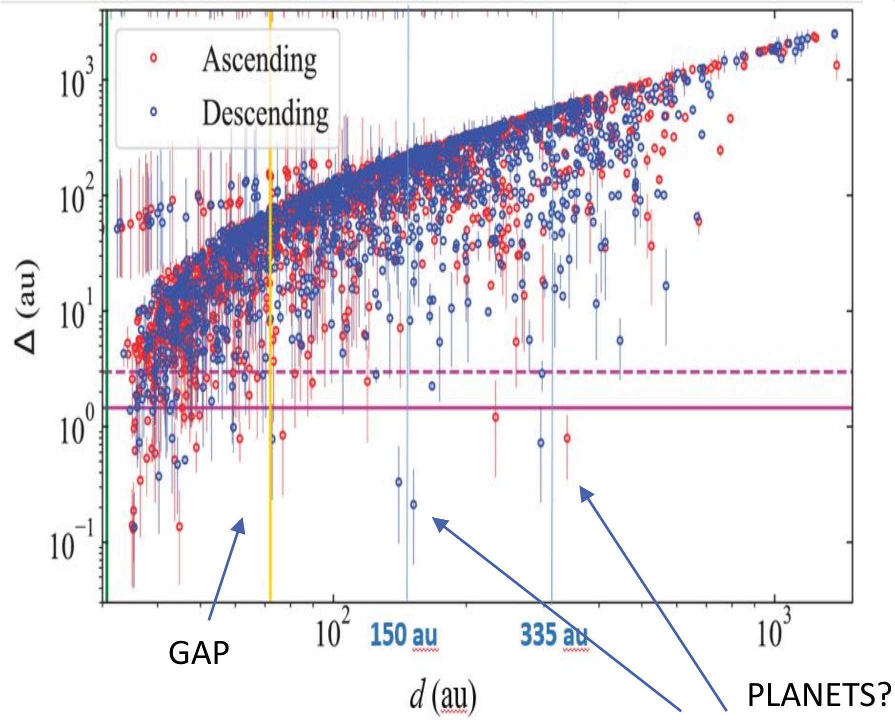

ATIRAS

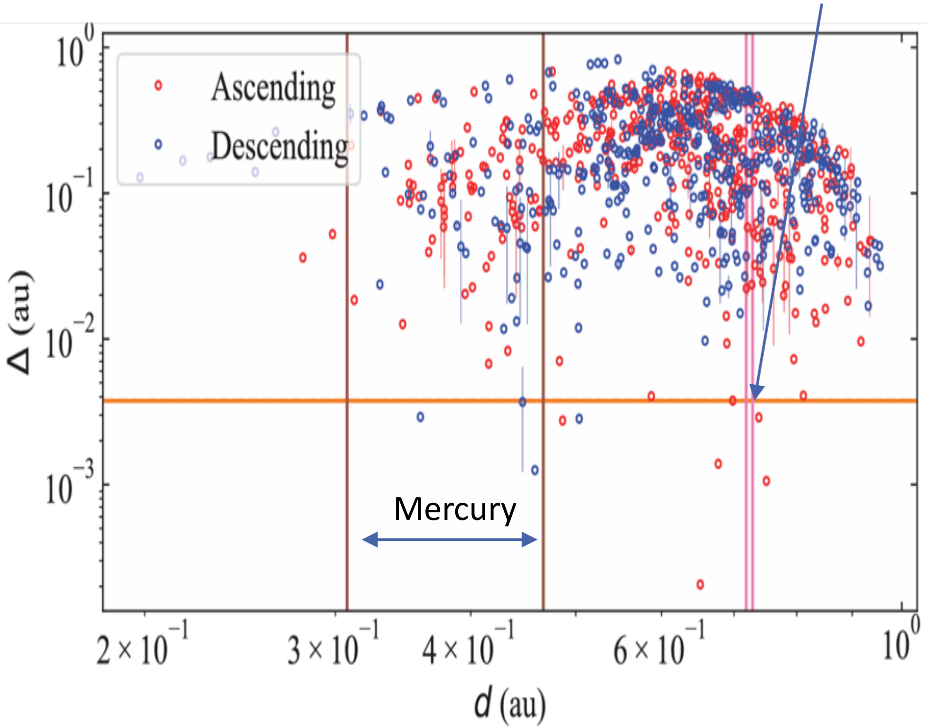

Origin of the Observed Substructure

Visible spectra of (474640) 2004 VN_{112}–2013 RF_{98} with OSIRIS at the 10.4 m GTC: evidence for binary dissociation near aphelion among the extreme trans-Neptunian objects

J. de León, C. de la Fuente Marcos, R. de la Fuente Marcos

Monthly Notices of the Royal Astronomical Society: Letters, Volume 467, Issue 1, May 2017, Pages L66–L70, https://doi.org/10.1093/mnrasl/slx003
Published: 07 January 2017 **Article history** ▾

PDF Split View Cite Permissions Share ▾

Abstract

The existence of significant anisotropies in the distributions of the directions of perihelia and orbital poles of the known extreme trans-Neptunian objects (ETNOs) has been used to claim that trans-Plutonian planets may exist. Among the known ETNOs, the pair (474640) 2004 VN_{112}–2013 RF_{98} stands out. Their orbital poles and the directions of their perihelia and their velocities at perihelion/aphelion are separated by a few degrees, but orbital similarity does not necessarily imply common physical origin. In an attempt to unravel their physical nature, visible spectroscopy of both targets was obtained using the OSIRIS camera-spectrograph at the 10.4 m Gran Telescopio Canarias (GTC). From the spectral analysis, we find that 474640–2013 RF_{98} have similar spectral slopes (12 versus 15 per cent/0.1 μm), very different from Sedna's but compatible with those of (148209) 2000 CR_{105} and 2012 VP_{113}. These five ETNOs belong to the group of seven linked to the Planet Nine hypothesis. A dynamical pathway consistent with these findings is dissociation of a binary asteroid during a close encounter with a planet and we

Close mutual nodal distances could be the result of binary disruption. High binary fraction for TNOs.